

15 The Geostrophic Momentum Approximation and the Semi-Geostrophic Equations in Isentropic Coordinates

15.1 Introduction

An emerging view in atmospheric dynamics is that the simplest way to diagnose or predict balanced flows is through the use of the Rossby-Ertel potential vorticity on isentropic surfaces. This is sometimes referred to as “IPV thinking” or “IPV modeling”. While it is true that the use of isentropic coordinates and the Rossby-Ertel potential vorticity dates back about sixty years (Rossby, 1937, 1940; Montgomery, 1937; Ertel, 1942), the modern view has added much—most notably the concepts of balance, invertibility and transformed horizontal coordinates. The modern view involves two main mathematical principles—the potential vorticity conservation principle as the prediction equation and the invertibility principle as the diagnostic equation to obtain the balanced wind and mass fields from the potential vorticity field. IPV thinking can lead to increased insight into such phenomena as the formation of cutoff cyclones and blocking anticyclones, Rossby wave propagation, and baroclinic/barotropic instability.

An important advantage to be exploited here is that which is gained by using IPV modeling in conjunction with certain horizontal coordinate transformations. This advantage is gained when the IPV approach is used with a filtered model which includes horizontal advection by the ageostrophic part of the wind. In such situations the proper choice of transformed horizontal coordinates can make this ageostrophic advection entirely implicit, which eliminates the need to solve an additional elliptic equation.

How do we handle situations where the lower boundary is not an isentropic surface? The simplest prototype problem to treat in this regard is probably the classic problem of surface frontogenesis by a vertically independent deformation field. In this chapter we show how the semi-geostrophic equations in isentropic coordinates can handle surface frontogenesis in a convenient and accurate fashion.

This chapter is organized as follows. Section 15.2 reviews the semi-geostrophic equations in isentropic coordinates, and the invertibility principle in geostrophic space is derived in section 15.3. In section 15.4 we show how to extend the semi-geostrophic equations to the case where the lower boundary is not an isentropic surface by incorporating a massless layer. The equations developed are then used to solve classic two-dimensional frontogenesis problem in section 15.5, and concluding remarks are given in section 15.6.

15.2 Semi-geostrophic theory and the potential pseudo-density equation

We begin with the f -plane system of equations with the geostrophic momentum approximation. Assuming the flow is frictionless and adiabatic, and using potential temperature as the vertical coordinate, our system becomes

$$\frac{Du_g}{Dt} - fv + \frac{\partial M}{\partial x} = 0, \quad (15.1)$$

$$\frac{Dv_g}{Dt} + fu + \frac{\partial M}{\partial y} = 0, \quad (15.2)$$

$$\frac{\partial M}{\partial \theta} = \Pi, \quad (15.3)$$

$$\frac{D\sigma}{Dt} + \sigma \left(\frac{\partial u}{\partial x} + \frac{\partial v}{\partial y} \right) = 0, \quad (15.4)$$

where

$$(fv_g, -fu_g) = \left(\frac{\partial M}{\partial x}, \frac{\partial M}{\partial y} \right) \quad (15.5)$$

define the components of geostrophic velocity, (u, v) are the horizontal components of the total velocity, $\Pi = c_p(p/p_0)^\kappa$ is the Exner function, $M = \theta\Pi + \phi$ the Montgomery potential with ϕ the geopotential, $\sigma = -\partial p/\partial \theta$ the pseudo-density, and

$$\frac{D}{Dt} = \frac{\partial}{\partial t} + u\frac{\partial}{\partial x} + v\frac{\partial}{\partial y} \quad (15.6)$$

the material derivative.

As shown in Appendix G, by combining x and y partial derivatives of (15.1) and (15.2), one can derive the equation

$$\frac{D\zeta}{Dt} + \zeta \left(\frac{\partial u}{\partial x} + \frac{\partial v}{\partial y} \right) = 0, \quad (15.7)$$

for the quantity

$$\zeta = f + \frac{\partial v_g}{\partial x} - \frac{\partial u_g}{\partial y} + \frac{1}{f} \frac{\partial(u_g, v_g)}{\partial(x, y)}, \quad (15.8)$$

which we refer to as the isentropic absolute vorticity, in view of (15.7). We can eliminate the isentropic divergence between (15.4) and (15.7) to obtain

$$\frac{D\sigma^*}{Dt} = 0, \quad (15.9)$$

where

$$\sigma^* = \frac{f}{\zeta} \sigma \quad (15.10)$$

is the potential pseudo-density. According to (15.10) the potential pseudo-density involves the wind field ζ and the mass field σ . Since ζ can be expressed in terms of u_g and v_g and hence M through geostrophic balance (15.5), and since σ can be expressed in terms of Π and hence M through hydrostatic balance (15.3), there exists a second-order partial differential equation relating M and σ^* . This equation, along with its associated boundary conditions, is usually referred to as the invertibility principle. Thus, we have (15.9) as a predictive equation for σ^* and an associated invertibility principle from which we can diagnose M from a known σ^* . However, when D/Dt is expressed in physical space by (15.6), (15.9) involves advection by the total wind, in which case the predictive equation for σ^* and the invertibility principle do not form a closed system. This is the point at which geostrophic coordinates $(X, Y, \Theta, T) = (x + v_g/f, y - u_g/f, \theta, t)$ enter the picture. The transformation to geostrophic coordinates makes the horizontal advecting velocity geostrophic, so that (15.9) becomes

$$\frac{\partial \sigma^*}{\partial T} + u_g \frac{\partial \sigma^*}{\partial X} + v_g \frac{\partial \sigma^*}{\partial Y} = 0, \quad (15.11)$$

which is the fundamental predictive equation of the model. Because the prediction of σ^* is then performed in geostrophic coordinate space, the invertibility principle must also be formulated in this space.

15.3 Invertibility principle in geostrophic space

Introducing the Bernoulli function $M^* = M + \frac{1}{2}(u_g^2 + v_g^2)$, it can be shown that the geostrophic and hydrostatic relations in (X, Y, Θ) take the form

$$(fv_g, -fu_g, \Pi) = \left(\frac{\partial M^*}{\partial X}, \frac{\partial M^*}{\partial Y}, \frac{\partial M^*}{\partial \Theta} \right), \quad (15.12)$$

which is identical to the form taken in (x, y, θ) . To prove the first entry, note that

$$\begin{aligned} \frac{\partial M}{\partial X} &= \frac{\partial M}{\partial x} \frac{\partial x}{\partial X} + \frac{\partial M}{\partial y} \frac{\partial y}{\partial X} \\ &= v_g \frac{\partial(fx)}{\partial X} - u_g \frac{\partial(fy)}{\partial X} \\ &= v_g \frac{\partial(fX - v_g)}{\partial X} - u_g \frac{\partial(fY + u_g)}{\partial X} \\ &= fv_g - v_g \frac{\partial v_g}{\partial X} - u_g \frac{\partial u_g}{\partial X}, \end{aligned}$$

where the geostrophic relations and the geostrophic coordinate definitions have been used. Taking the last two terms over to the left hand side, we obtain $\partial M^*/\partial X = fv_g$, which is the first entry in (15.12). The second and third entries in (15.12) can be obtained in a similar manner.

Also, the isentropic vorticity in (X, Y, Θ) takes the form

$$\frac{f}{\zeta} = \frac{\partial(x, y)}{\partial(X, Y)} = 1 - \frac{1}{f} \left(\frac{\partial v_g}{\partial X} - \frac{\partial u_g}{\partial Y} \right) + \frac{1}{f^2} \frac{\partial(u_g, v_g)}{\partial(X, Y)}. \quad (15.13)$$

Thus, σ^* depends only on M^* , and we again conclude that the wind and mass fields can in principle be obtained from σ^* if we can somehow invert it to obtain M^* .

The relation between M^* and σ^* is derived as follows. From the definition of σ^* and (15.13) we have

$$\frac{\partial(x, y, \Pi)}{\partial(X, Y, \Theta)} + \Gamma \sigma^* = 0, \quad (15.14)$$

where $\Gamma = d\Pi/dp = \kappa\Pi/p$. Expressing x and y in terms of u_g and v_g , and then using (15.12), we can write (15.14) as

$$\frac{1}{f^4} \begin{vmatrix} \frac{\partial^2 M^*}{\partial X^2} - f^2 & \frac{\partial^2 M^*}{\partial Y \partial X} & \frac{\partial^2 M^*}{\partial \Theta \partial X} \\ \frac{\partial^2 M^*}{\partial X \partial Y} & \frac{\partial^2 M^*}{\partial Y^2} - f^2 & \frac{\partial^2 M^*}{\partial \Theta \partial Y} \\ \frac{\partial^2 M^*}{\partial X \partial \Theta} & \frac{\partial^2 M^*}{\partial Y \partial \Theta} & \frac{\partial^2 M^*}{\partial \Theta^2} \end{vmatrix} + \Gamma \sigma^* = 0. \quad (15.15a)$$

If the upper boundary is an isentropic surface with potential temperature Θ_T and the Exner function Π_T —or equivalently the pressure p_T —is specified there (e.g., constant for an isobaric top), the upper boundary condition for (15.15a) is simply

$$\frac{\partial M^*}{\partial \Theta} = \Pi_T \quad \text{at} \quad \Theta = \Theta_T. \quad (15.15b)$$

Likewise, if the lower boundary condition is the isentropic surface $\Theta = \Theta_B$ and the surface geopotential ϕ_S is specified there (e.g., $\phi_S = 0$ for a flat lower boundary), then $M = \Theta\Pi + \phi_S$ at $\Theta = \Theta_B$. Written in terms of M^* , this lower boundary condition becomes

$$M^* - \Theta \frac{\partial M^*}{\partial \Theta} - \frac{1}{2f^2} \left[\left(\frac{\partial M^*}{\partial X} \right)^2 + \left(\frac{\partial M^*}{\partial Y} \right)^2 \right] = \phi_S \quad \text{at} \quad \Theta = \Theta_B. \quad (15.15c)$$

Together with appropriate lateral boundary conditions, equations (15.11), (15.12) and (15.15) form a closed system. The computational scheme is as follows: knowing σ^* , solve (15.15) for M^* ; use (15.12) to compute u_g and v_g ; use these geostrophic winds in (15.11) to predict a new σ^* . However, to make the system useful for modeling realistic flows we must relax the assumption of an isentropic lower boundary.

15.4 The massless layer approach

To apply the semi-geostrophic equations when the lower boundary is not necessarily an isentropic surface, we adopt an approach which has proved useful in such contexts as the definition of available potential energy (Lorenz, 1955), the analysis of baroclinic instability (Bretherton, 1966; Hoskins et al., 1985; James and Hoskins, 1985; Hsu and Arakawa, 1990), and the finite amplitude Eliassen-Palm theorem (Andrews, 1983). The key idea is to think of an isentropic surface which intersects the earth's surface as continuing just under the earth's surface with a pressure equal to the surface pressure. At any horizontal position where two distinct isentropic surfaces run just under the earth's surface (and hence have the same pressure), there is no mass trapped between them, so that $\sigma^* = \sigma = 0$ there. This "massless layer" approach is consistent with Bretherton's (1966) conclusion that "any flow with potential temperature variations over a horizontal rigid plane boundary may be considered equivalent to a flow without such variations, but with a concentration of potential vorticity very close to the boundary." We have simply replaced Bretherton's thin sheet of infinite potential vorticity with a thin sheet of zero potential pseudo-density.

We extend the semi-geostrophic equations to the massless layer as follows. We first let the surface geopotential and potential temperature be given by $\phi_S(x, y, t)$ and $\theta_S(x, y, t)$, respectively, so that

$$\phi(x, y, \theta_S(x, y, t), t) = \phi_S(x, y, t), \quad (15.16)$$

and define ϕ and p for $\theta < \theta_S$ by

$$\phi(x, y, \theta, t) = \phi_S(x, y, t), \quad p(x, y, \theta, t) = p_S(x, y, t) \equiv p(x, y, \theta_S, t). \quad (15.17)$$

From the definitions of σ , Π , and M we then obtain

$$\sigma = 0, \quad \Pi = \Pi_S \equiv \Pi(p_S), \quad M = \theta \Pi_S + \phi_S \quad (15.18)$$

for $\theta < \theta_S$. We note that p , Π , and M are continuous at $\theta = \theta_S$, but σ jumps discontinuously from $\sigma = 0$ for $\theta < \theta_S$ to $\sigma > 0$ for $\theta > \theta_S$. Also, p and Π are constant in the massless layer, while M varies linearly with θ there. From (15.18) we see that the hydrostatic relation (15.3) holds for $\theta < \theta_S$; a careful analysis shows that it also holds at $\theta = \theta_S$. Then defining (u_g, v_g) for $\theta < \theta_S$ by (15.5) and defining (u, v) so that (15.1) and (15.2) hold in the massless layer completes the extension of semi-geostrophic theory. Since the governing equations and definitions all apply unchanged in the massless layer, the derivation of the potential pseudo-density equation, the transformation to geostrophic coordinates, and the derivation of the invertibility principle all proceed exactly as in section 15.2 and section 15.3.

We thus conclude that (15.11), (15.12), and (15.15) are valid in the massless layer. The lower boundary condition (15.15c) is in fact valid anywhere that $\Theta_B \leq \Theta_S$ holds; for convenience, we choose a constant value Θ_B which satisfies this constraint everywhere, and apply (15.15c) at Θ_B rather than at Θ_S . We then predict the evolution of the entire σ^* field (including the zero potential pseudo-density region) with (15.11). Of course, $\sigma^* = 0$ in the massless layer, but the boundary of the region may move. Since this boundary is the surface potential temperature, i.e., that value of Θ at which σ^* jumps from zero to a positive value, this procedure also predicts Θ_S . Any numerical method used to solve (15.11) must cope properly with the discontinuity in σ^* at Θ_S . However, workable schemes do exist. For example, recently Arakawa and Hsu (1990), in the context of solving (15.4) in a primitive equation model, have proposed a finite difference scheme which has very small dissipation and computational dispersion and which guarantees positive definiteness. Note, however, that the discontinuity in σ^* presents less of a problem in solving (15.15) numerically, since σ^* plays the role of the forcing, rather than the solution, and is not differentiated.

15.5 Frontogenesis by horizontal deformation fields

Let us now reconsider the two-dimensional frontogenesis problem of Hoskins (1971, 1972) and Hoskins and Bretherton (1972). Fronts oriented in the y -direction are assumed to be forced by a pure deformation field so that

$$u_g(x, y, \theta, t) = -\alpha x, \quad (15.19a)$$

$$v_g(x, y, \theta, t) = \alpha y + v'_g(x, \theta, t), \quad (15.19b)$$

with the first terms on the right hand side representing the fixed (or “slowly” varying) deformation field and the v'_g term representing the rotational flow generated during the frontogenesis. Assuming σ^* is independent of y so that

$$\frac{\partial \sigma^*}{\partial y} = \frac{\partial X}{\partial y} \frac{\partial \sigma^*}{\partial X} + \frac{\partial Y}{\partial y} \frac{\partial \sigma^*}{\partial Y} = 0 \quad (15.20)$$

and using the definitions of (X, Y) and the assumptions (15.19) we obtain

$$\frac{\partial \sigma^*}{\partial Y} = -\frac{\alpha}{f} \frac{\partial \sigma^*}{\partial X}. \quad (15.21)$$

Using this result in (15.11), we obtain

$$\frac{\partial \sigma^*}{\partial T} - \alpha X \frac{\partial \sigma^*}{\partial X} = 0. \quad (15.22)$$

The solution of (15.22) is given by

$$\sigma^*(X, \Theta, T) = \sigma^*(X e^{\alpha T}, \Theta, 0). \quad (15.23)$$

For the initial condition we assume that σ^* takes on the constant value σ_T in the top part, the larger constant value σ_B in the bottom part, and a zero value in the massless region of the model atmosphere. These three regions are separated by the tropopause interface potential temperature $\theta_I(x)$ and the surface potential temperature $\theta_S(x)$. To allow the possibility of smoothing discontinuous jumps in σ^* over small ranges specified by $\Delta\theta_S$ and $\Delta\theta_I$ we set

$$\sigma^*(x, \theta, 0) = \frac{1}{2} \left[\sigma_T + \sigma_B \tanh \left(\frac{\theta - \theta_S}{\Delta\theta_S} \right) - (\sigma_B - \sigma_T) \tanh \left(\frac{\theta - \theta_I}{\Delta\theta_I} \right) \right], \quad (15.24)$$

which reduces to

$$\sigma^*(x, \theta, 0) = \begin{cases} \sigma_T, & \theta_I(x, 0) < \theta \leq \theta_T \\ \sigma_B, & \theta_S(x, 0) < \theta < \theta_I(x, 0) \\ 0, & \theta_B \leq \theta < \theta_S(x, 0) \end{cases} \quad (15.25)$$

in the limit as $\Delta\theta_S \rightarrow 0$ and $\Delta\theta_I \rightarrow 0$. If the x -derivatives of $\theta_S(x, 0)$ and $\theta_I(x, 0)$ are sufficiently small, the relative vorticity associated with this initial σ^* field will be much less than f and σ^* will approximately equal σ . Then we can integrate (15.24) from θ_B to θ_T to obtain

$$p_S(x, 0) - p_T = \frac{1}{2} [\sigma_T(\theta_T - \theta_B) + \sigma_B A_S - (\sigma_B - \sigma_T) A_I], \quad (15.26a)$$

where

$$A_S = \Delta\theta_S \ln \left\{ \frac{\cosh[(\theta_T - \theta_S)/\Delta\theta_S]}{\cosh[(\theta_B - \theta_S)/\Delta\theta_S]} \right\} \quad (15.26b)$$

and

$$A_I = \Delta\theta_I \ln \left\{ \frac{\cosh[(\theta_T - \theta_I)/\Delta\theta_I]}{\cosh[(\theta_B - \theta_I)/\Delta\theta_I]} \right\}. \quad (15.26c)$$

We note that $A_S \rightarrow \theta_T - 2\theta_S + \theta_B$ as $\Delta\theta_S \rightarrow 0$ and $A_I \rightarrow \theta_T - 2\theta_I + \theta_B$ as $\Delta\theta_I \rightarrow 0$. If $\sigma_T \neq \sigma_B$ then (15.26) determines the interface potential temperature θ_I (this must be computed numerically if $\Delta\theta_I > 0$); otherwise, there is no interface, and (15.26) serves as a constraint on the common value $\sigma_T = \sigma_B$.

For the initial surface potential temperature we specify

$$\theta_S(x, 0) = \theta_B + \Delta\theta \left[1 + \tanh\left(\frac{x}{L}\right) \right], \quad (15.27)$$

and specify the initial surface pressure $p_S(x, 0) = p_B = \text{constant}$. Here we use the values $\sigma_B = 8\sigma_T = 2 \text{ kPa/K}$, $p_T = 5 \text{ kPa}$, $\theta_T = 400 \text{ K}$, $p_B = 100 \text{ kPa}$, $\theta_B = 265 \text{ K}$, and $\Delta\theta = 17.5 \text{ K}$. Figure 15.1a shows the initial (analytical) θ field as a function of x and p with $\Delta\theta_I = 5 \text{ K}$ and $\Delta\theta_S = 0 \text{ K}$; part (b) shows the corresponding initial σ^* field (15.24) as a function of X and Θ (the smoothing at the tropopause is not shown). Since $\sigma_B/(\sigma_B - \sigma_T) = 8/7$, the potential temperature variation on the tropopause is slightly larger than the potential temperature variation at the surface. According to (15.23) the two boundaries between the three σ^* regions simply steepen as frontogenesis proceeds.

The structure of the evolving front was computed at several values of αt by evaluating the potential pseudo-density σ^* analytically from (15.23) and (15.24), and then solving the invertibility relation numerically as follows. With the assumption of y -independence, (15.15) reduces to a two-dimensional problem in X and Θ [c.f. (15.21)]. Although X is scaled by the factor $\sqrt{1 + \alpha^2/f^2}$, assuming that the deformation field is weak (i.e., $\alpha \ll f$), this factor may be dropped. The lower boundary is taken to be flat ($\phi_S = 0$) and the top isobaric ($p = p_T$). A 256×32 grid was used, covering the domain $-4 \leq X/L \leq 4$ shown in Fig. 15.1. At the lateral boundaries M^* was computed by assuming it to be independent of X , and solving (15.15) as a boundary value problem in Θ only. For clarity, only the central portion $-1 \leq X/L \leq 1$ of the computational domain is shown in the subsequent figures.

Figure 15.2 shows the front at $\alpha t = 1$. Part (a) shows the potential pseudo-density σ^* evaluated on the computational grid, part (b) shows the wind (v_g) and mass (p) fields in the geostrophic/isentropic coordinates (X, Θ), and part (c) shows the wind (v_g) and mass (θ) fields in the physical coordinates (x, p). A dotted line on each figure indicates the earth's surface (θ_S or p_S). It is interesting to note that the fields in the massless layer (Fig. 15.2b) satisfy the assumptions given in section 15.4, even though these assumptions were not incorporated into the numerical solver. Corresponding results at a later time ($\alpha t = 2$) in Fig. 15.3 show the surface front and corresponding upper-tropospheric jet strengthening.

An interesting feature of the semi-geostrophic system is that it predicts the development of a true discontinuity in finite time (Hoskins and Bretherton, 1972). This result is also obtained in the isentropic coordinate formulation employed here. Figure 15.4 shows the computed structure of the front at $\alpha t = 3$. However, the transformation from geostrophic (X) to physical (x) coordinates has broken down at this time, so the fields shown in Fig. 15.4c contain some error. This is most clearly seen in Fig. 15.5, which shows x as a function of X ; note that at the surface, θ has become a multiple-valued function of x , so in fact a true discontinuity has developed. In the real atmosphere, of course, physical processes neglected in this study (e.g., friction or Kelvin-Helmholtz instability along the front) would

become significant before this time; this point is addressed in more detail in Hoskins and Bretherton (1972). Away from the surface discontinuity the computed fields at $\alpha t = 3$ should be approximately correct; we see in Fig. 15.6 that the model has begun to develop the folded tropopause characteristic of strong fronts in the real atmosphere (Shapiro et al., 1987). The low-level minimum of σ^* in Fig. 15.6 is an artifact of the coordinate transformation, which has broken down near the surface front.

15.6 Concluding remarks

We have now seen that the most concise version of f -plane semi-geostrophic theory is that version which makes simultaneous use of isentropic and geostrophic coordinates. The use of isentropic coordinates for adiabatic flow simplifies the material derivative operator to (15.6), while the use of geostrophic coordinates further simplifies the horizontal advection by making it geostrophic. The fundamental predictive equation for potential pseudo-density then takes the simple form (15.11), and the invertibility principle (15.15) closes the theory. This basic structure of a closed theory based on a predictive equation for σ^* and an invertibility principle for M^* is maintained in the β -plane and hemispheric generalizations of semi-geostrophic theory. The combined use of isentropic and generalized geostrophic coordinates is crucial for the mathematical simplicity of these β -plane and hemispheric semi-geostrophic theories.

Problems

1. Prove that, in the two-dimensional frontogenesis case, the invertibility relation (15.15a) reduces to

$$-\frac{1}{f^2} \left\{ \left[\left(1 + \frac{\alpha^2}{f^2} \right) \frac{\partial^2 M^*}{\partial X^2} - f^2 \right] \frac{\partial^2 M^*}{\partial \Theta^2} - \left(1 + \frac{\alpha^2}{f^2} \right) \left(\frac{\partial^2 M^*}{\partial X \partial \Theta} \right)^2 \right\} + \Gamma \sigma^* = 0.$$

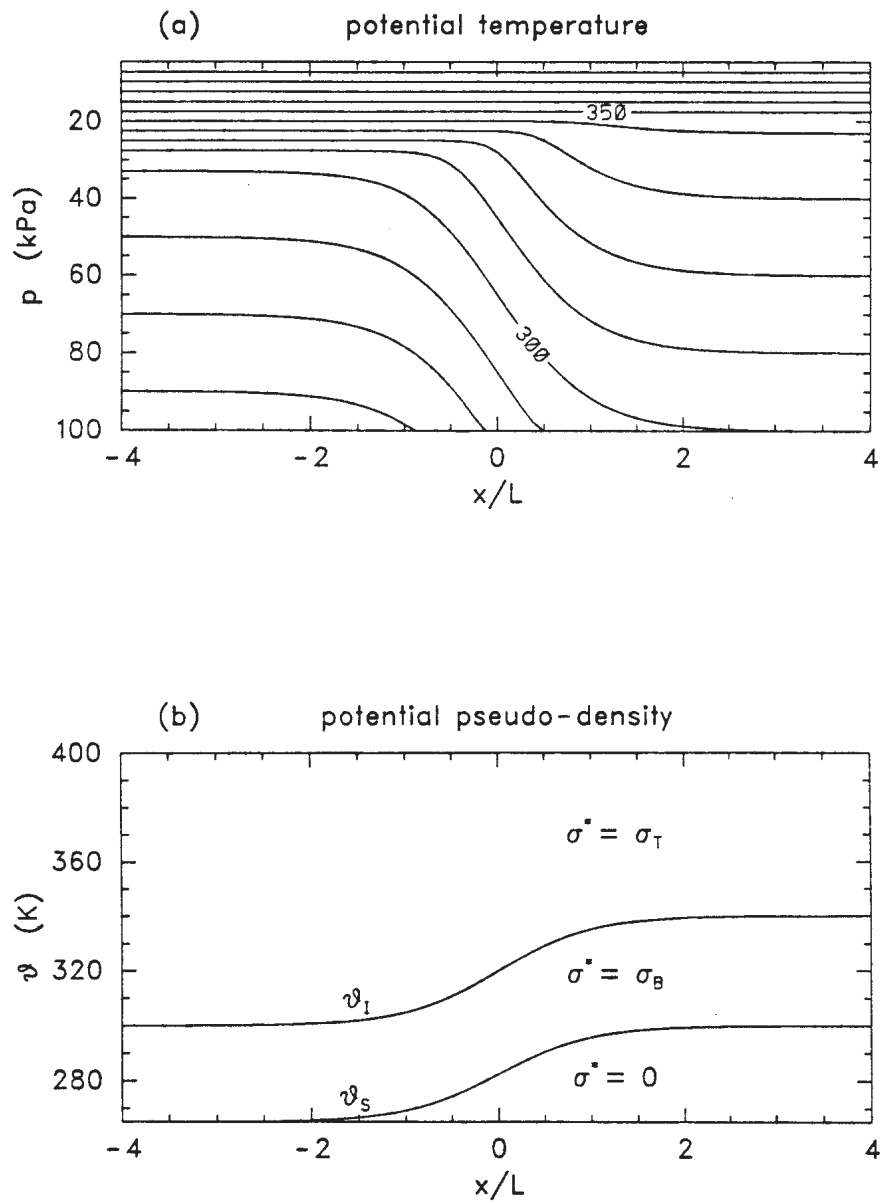


Figure 15.1: (a) Initial ($\alpha t = 0$) θ field in (x, p) space; (b) Corresponding initial σ^* field in (x, θ) -space.

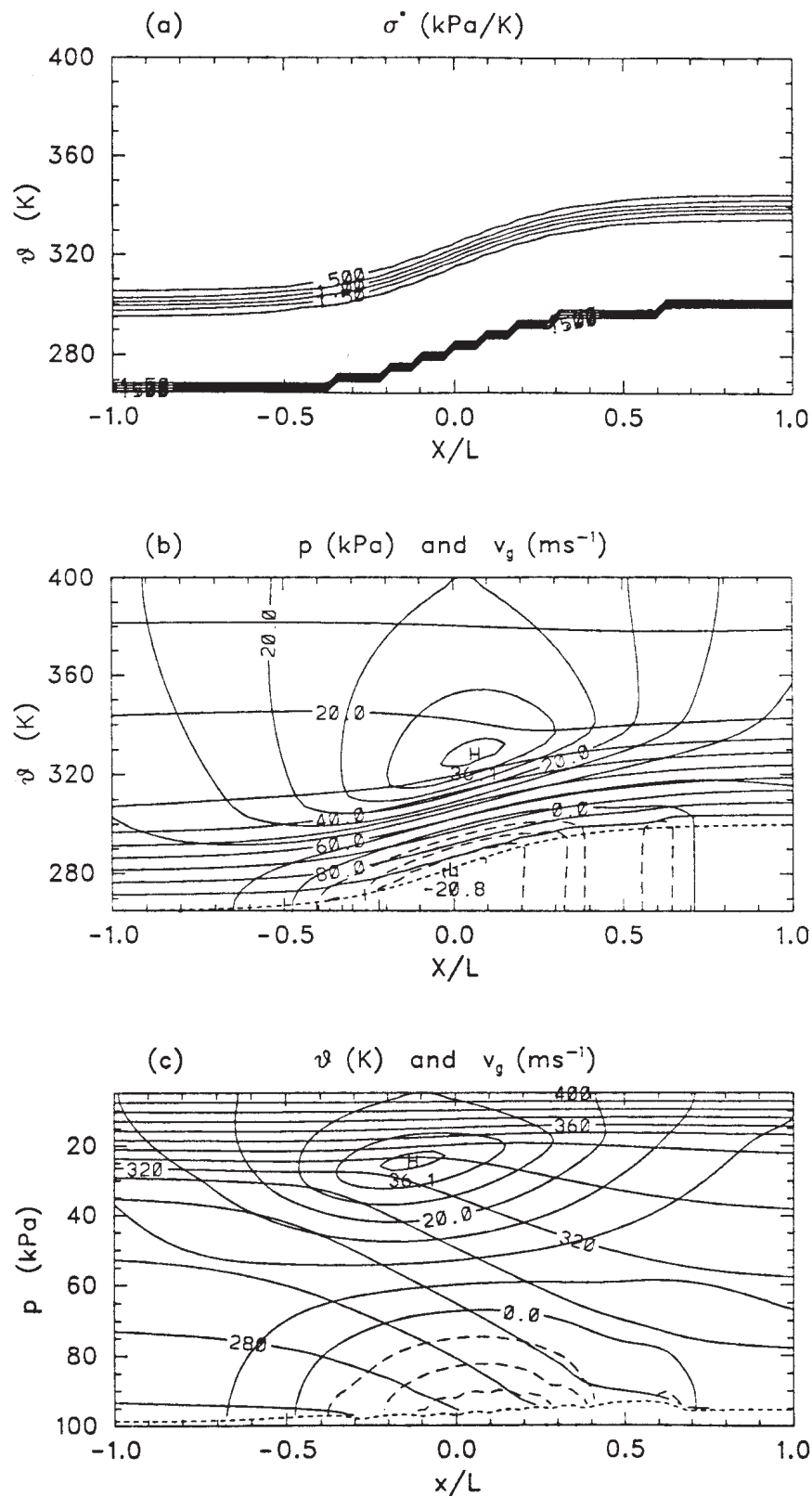


Figure 15.2: Structure of the front at $\alpha t = 1$: (a) σ^* in (x, p) -space, (b) p and v_g in (X, Θ) -space, and (c) θ and v_g in (x, p) -space. Dashed contours represent $v_g < 0$ (out of the paper) and dotted lines represent the earth's surface. Note the change in the X scale from Fig. 15.1. 15-8

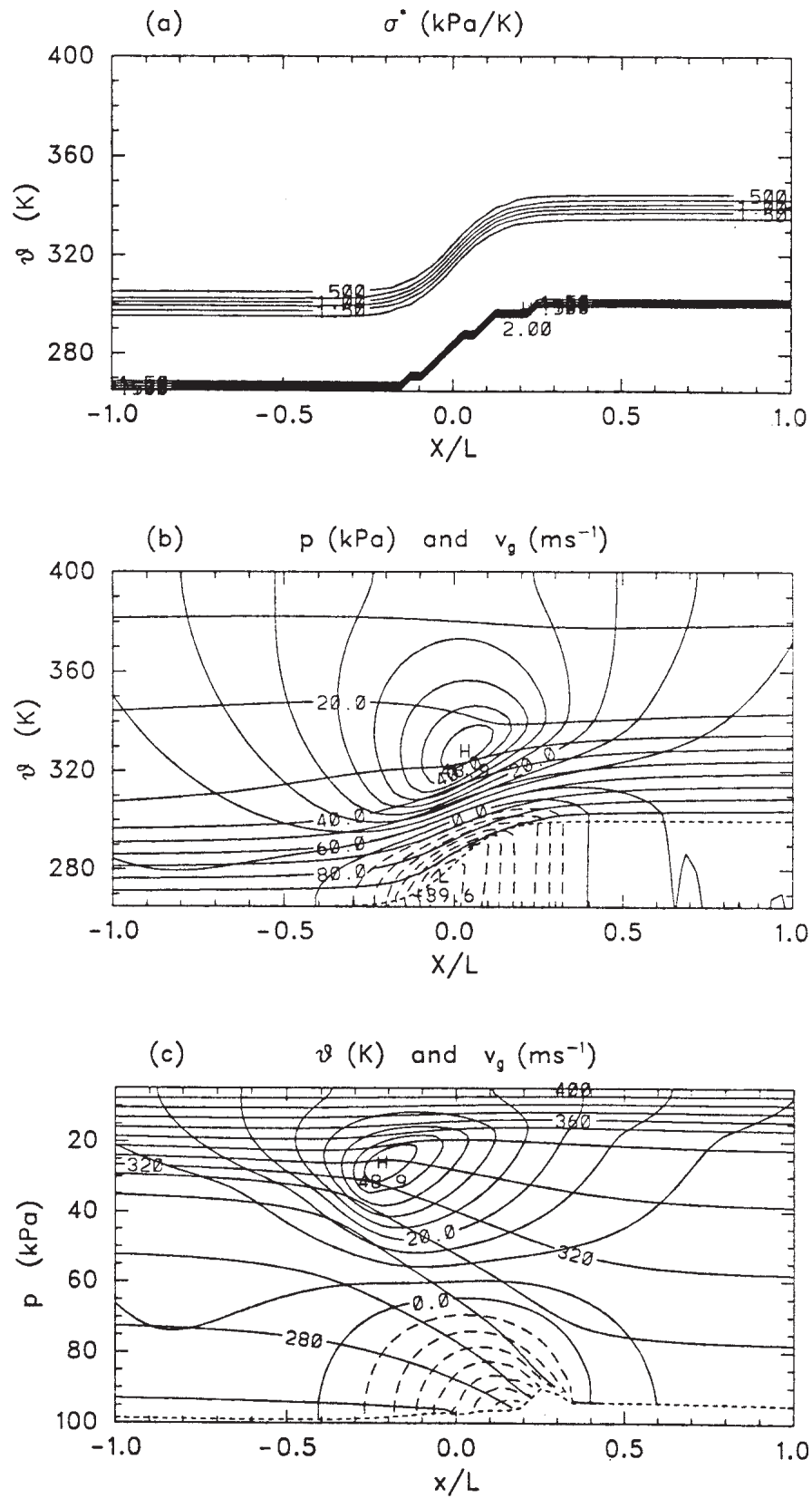


Figure 15.3: Same as Fig. 15.2 except at $\alpha t = 2$.

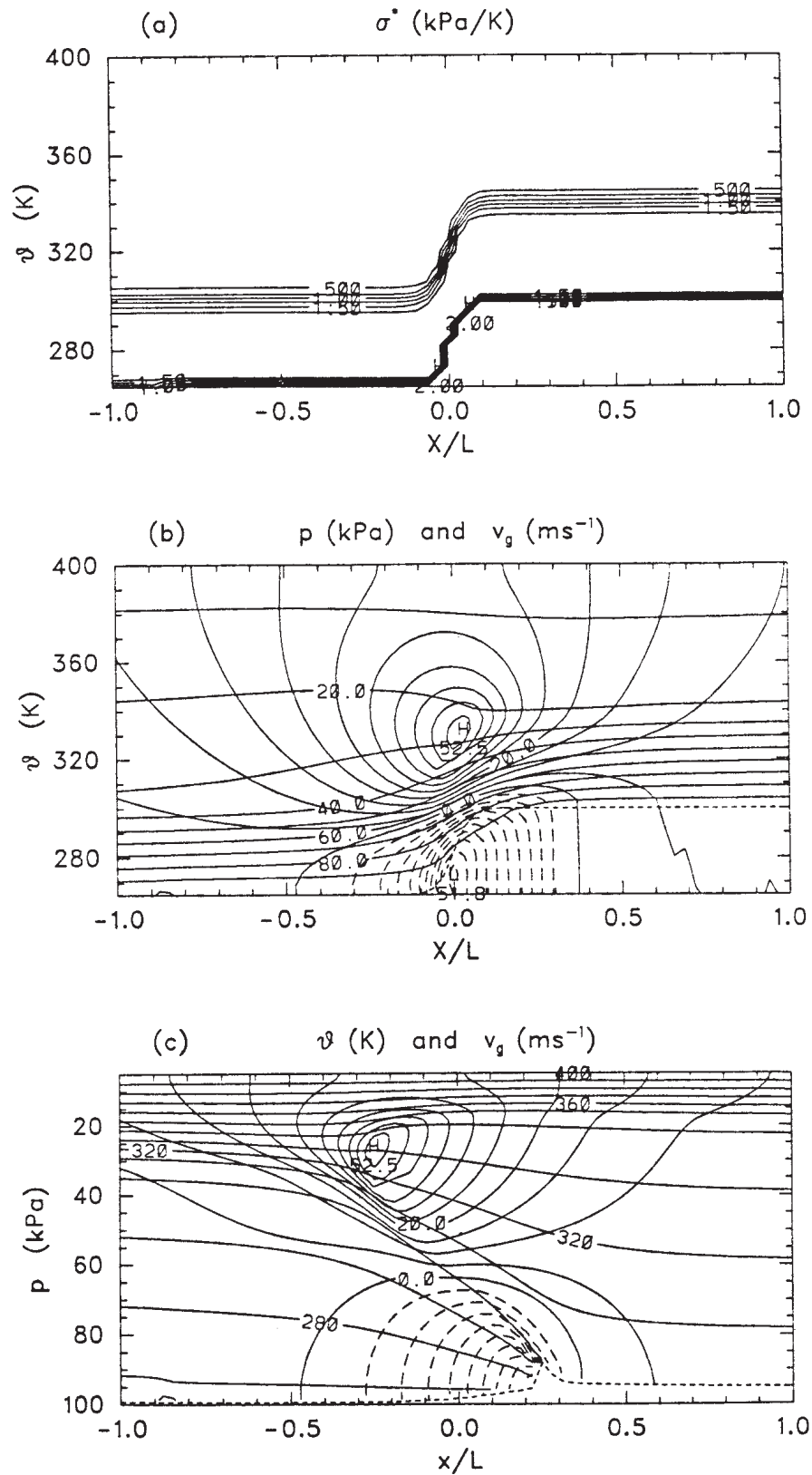


Figure 15.4: Same as Fig. 15.2 except at $\alpha t = 3$.

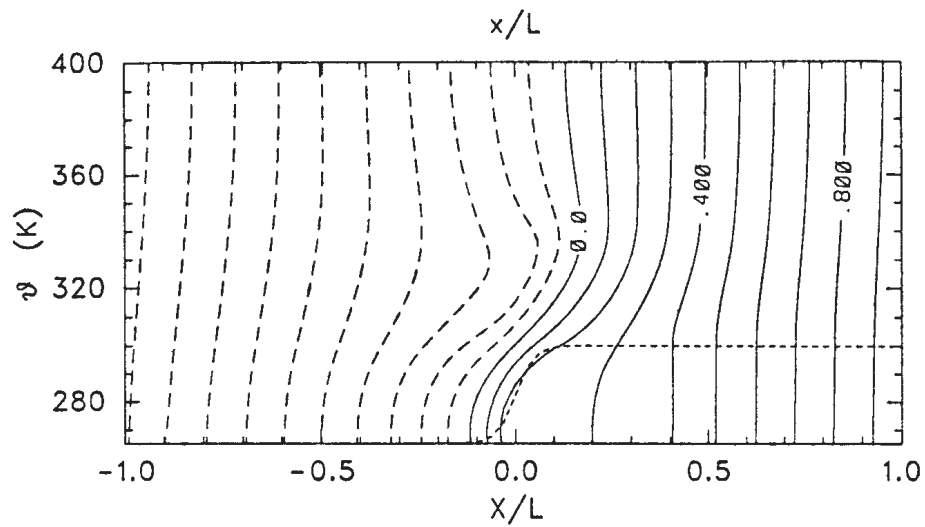


Figure 15.5: Physical coordinate x/L in (X, Θ) -space at $\alpha t = 3$.

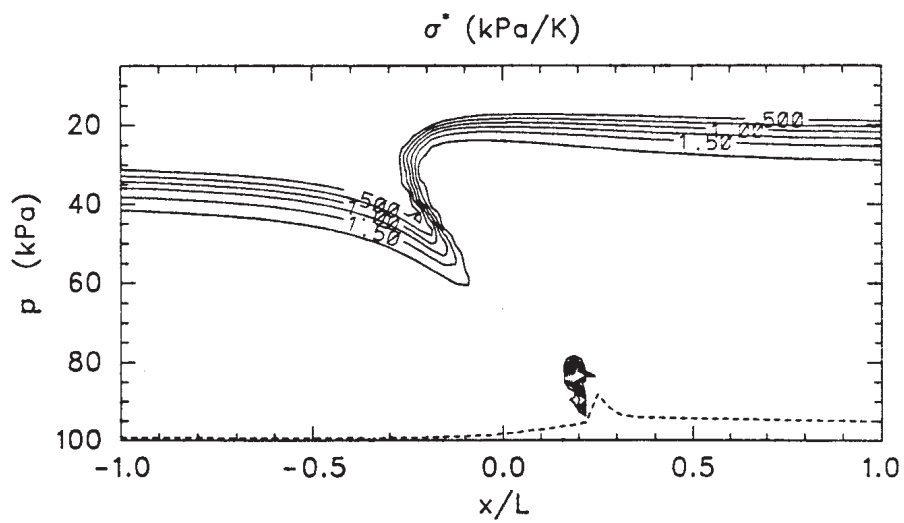


Figure 15.6: Potential pseudodensity (inverse potential vorticity) σ^* in (x, p) -space at $\alpha t = 3$.

15.7 Historical notes and references

Two ideas which underlie most of our discussion are the geostrophic momentum approximation and the transformation to geostrophic coordinates in the horizontal or isentropic coordinates in the vertical. The geostrophic momentum approximation was first briefly discussed by Eliassen, not so much with the goal of producing a theoretical model but rather of introducing a formula from which the wind could be calculated using geopotential observations.

- Eliassen, A., 1948: The quasi-static equations of motion. *Geofys. Publ.*, **17**, No. 3.

Later, Fjørtoft studied the geostrophic momentum approximation with the goal of eventual numerical solutions. Although Fjørtoft did not use geostrophic coordinates, he did realize the advantage of vertical derivatives along the absolute vorticity vector. He also recognized that the geostrophic momentum approximation and the quasi-geostrophic approximation should give similar results except for horizontal distortions and vertical tilts.

- Fjørtoft, R., 1962: On the integration of a system of geostrophically balanced prognostic equations. *Proc. Int. Symp. Numerical Weather Prediction*, Meteorological Society of Japan, 153–159.
- Fjørtoft, R., and B. Söderberg, 1965: A prediction experiment with filtered equations. NCAR Manuscript No. 59, 33 pp.

Geostrophic coordinates were apparently first introduced by Yudin.

- Yudin, M. I., 1955: Invariant quantities in large-scale atmospheric processes. *Tr. Glav. Geofiz. Observ.*, No. 55, 3–12.

The paper by Yudin is in Russian but an English summary can be found in Phillips et al.

- Phillips, N. A., W. Blumen, and O. R. Coté, 1960: Numerical weather prediction in the Soviet Union. *Bull. Amer. Meteor. Soc.*, **41**, 599–617.

Yudin apparently did not make use of the geostrophic momentum approximation. The first use of the geostrophic coordinate in the western literature was by Eliassen in his study of the two-dimensional vertical circulation in frontal zones. This paper gives the two-dimensional version of (14.70) and (14.71).

The first exploitation of both the geostrophic momentum approximation and the geostrophic coordinate was in the two-dimensional frontogenesis studies of Hoskins (1971) and Hoskins and Bretherton (1972).

- Hoskins, B. J., 1971: Atmospheric frontogenesis: some solutions. *Quart. J. Roy. Meteor. Soc.*, **97**, 139–153.
- Hoskins, B. J., and F. P. Bretherton, 1972: Atmospheric frontogenesis models: mathematical formulation and solution. *J. Atmos. Sci.*, **29**, 11–37.

Later, a comprehensive semi-geostrophic theory in three dimensions was worked out by Hoskins (1975) and Hoskins and Draghici (1977). These papers should be read as a pair to understand the complete theory.

- Hoskins, B. J., 1975: The geostrophic momentum approximation and the semi-geostrophic equations. *J. Atmos. Sci.*, **32**, 233–242.
- Hoskins, B. J., and I. Draghici, 1977: The forcing of ageostrophic motion according to the semi-geostrophic equations and in an isentropic coordinate model. *J. Atmos. Sci.*, **34**, 1859–1867.

At the time the first paper was written the forms of the generalized omega equation and the generalized Eliassen cross-front circulation equation were apparently not known. Since the generalized omega equation is written with the forcing as the divergence of the \mathbf{Q} -vector, the quasi-geostrophic omega equation can also be written this way. For a discussion of the quasi-geostrophic omega equation in terms of \mathbf{Q} -vectors, see

- Hoskins, B. J., I. Draghici, and H. C. Davies, 1978: A new look at the ω -equation. *Quart. J. Roy. Meteor. Soc.*, **104**, 31–38.

- Trenberth, K. E., 1978: On the interpretation of the diagnostic quasi-geostrophic omega equation. *Mon. Wea. Rev.*, **106**, 131–137.

Detailed studies of frontogenesis in semi-geostrophic models have been made by

- Hoskins, B. J., 1972: Non-Boussinesq effects and further development in a model of upper tropospheric frontogenesis. *Quart. J. Roy. Meteor. Soc.*, **98**, 532–541.
- Hoskins, B. J., 1974: The formation of atmospheric fronts downstream in a deformation field. *J. Fluid Mech.*, **64**, 177–194.
- Blumen, W., 1980: A comparison between the Hoskins-Bretherton model of frontogenesis and the analysis of an intense surface frontal zone. *J. Atmos. Sci.*, **37**, 64–77.

Imposing a horizontal deformation field is one way of forcing frontogenesis. A more realistic way is to start from a baroclinically unstable zonal flow and allow the developing baroclinic wave to force frontogenesis. In this regard Eady waves and uniform potential vorticity flows have been studied by

- Hoskins, B. J., 1976: Baroclinic waves and frontogenesis. Part I: Introduction and Eady waves. *Quart. J. Roy. Meteor. Soc.*, **102**, 103–122.
- Hoskins, B. J., and N. V. West, 1979: Baroclinic waves and frontogenesis. Part II: Uniform potential vorticity jet flows—cold and warm fronts. *J. Atmos. Sci.*, **36**, 1663–1680.
- Heckley, W. A., and B. J. Hoskins, 1982: Baroclinic waves and frontogenesis in a non-uniform potential vorticity semi-geostrophic model. *J. Atmos. Sci.*, **39**, 1999–2016.
- Blumen, W., 1978a: Uniform potential vorticity flow: Part I. Theory of wave interactions and two-dimensional turbulence. *J. Atmos. Sci.*, **35**, 774–783.
- Blumen, W., 1978b: Uniform potential vorticity flow: Part II. A model of wave interactions. *J. Atmos. Sci.*, **35**, 784–789.
- Blumen, W., 1979: Unstable nonlinear evolution of an Eady wave in time-dependent basic flows and frontogenesis. *J. Atmos. Sci.*, **36**, 3–11.

A study of the energy cascade predicted by the semi-geostrophic theory of frontogenesis can be found in

- Andrews, D. G., and B. J. Hoskins, 1978: Energy spectra predicted by semi-geostrophic theories of frontogenesis. *J. Atmos. Sci.*, **35**, 509–512.

An interpretation of geostrophic coordinates as a kind of contact transformation has been given by

- Blumen, W., 1981: The geostrophic coordinate transformation. *J. Atmos. Sci.*, **38**, 1100–1105.